PROCEEDINGS OF SCIENCE

NNLO QCD predictions for $t\bar{t}W$ production at the LHC

Xiang Chen[a,*]

[a] *Physik-Institut, Universität Zürich,*
Winterthurerstrasse 190, 8057 Zürich, Switzerland

E-mail: xiang.chen@physik.uzh.ch

The production of a top–antitop quark pair in association with a W boson ($t\bar{t}W$) is one of the heaviest signatures currently explored at the Large Hadron Collider (LHC) and the corresponding rates have been found to be consistently higher than the Standard Model predictions, highlighting the need for more accurate theoretical predictions. In this contribution, I present next-to-next-to-leading order (NNLO) predictions for this process, in which, for the first time, the necessary two-loop amplitudes are explicitly evaluated in the generalized leading-color limit.

Loops and Legs in Quantum Field Theory (LL2026)
12-17, April, 2026
Bayreuth, Germany

*Speaker

© Copyright owned by the author(s) under the terms of the Creative Commons Attribution-NonCommercial-NoDerivatives 4.0 International License (CC BY-NC-ND 4.0) All rights for text and data mining, AI training, and similar technologies for commercial purposes, are reserved. ISSN 1824-8039 . Published by SISSA Medialab.

PoS(LL2026)055

1. Introduction

The signature $pp \to t\bar{t}W$ stands out among LHC processes for being one of the heaviest that can be studied with current data. The top quark decays almost immediately ($t \to Wb$), so the final state contains a pair of b-jets together with three W bosons, translating into a rich multi-lepton topology once the W's decay leptonically. This feature places $t\bar{t}W$ among the key backgrounds for searches targeting new physics with multiple leptons, and makes it one of the rare SM channels that yield same-sign dilepton events [1–3]. At the parton level, the process proceeds at leading order via quark–antiquark annihilation of different flavours; consequently, the W is radiated exclusively from the initial-state light quarks, giving the cross section particular sensitivity to the quark PDFs. The process also receives contributions from both QCD and EW higher orders, so that multiple mass scales play a role simultaneously.

Experimental results have been collected by ATLAS and CMS at $\sqrt{s} = 8\,\text{TeV}$ [4, 5] and 13 TeV [6–12]. A recurring feature is that the measured inclusive rates lie above the SM expectation, with indirect hints pointing in the same direction from $t\bar{t}H$ [13, 14] and $t\bar{t}t\bar{t}$ [15, 16] measurements. This persistent tension calls for increasingly accurate theory.

On the theory front, much progress has been made over the past decade. On-shell NLO QCD predictions became available first [17–19], followed by the inclusion of EW corrections [20, 21]. Soft-gluon effects have been pushed to NNLL accuracy [22–25]. The full off-shell framework, which retains decay kinematics, was developed at NLO initially in QCD [26–28] and subsequently extended to the combination of QCD and EW effects [29]. Multi-jet merging techniques have also been applied to these off-shell calculations [30, 31], and it is against these merged NLO QCD+EW results that most experimental analyses currently compare their data.

The path to NNLO accuracy for $t\bar{t}W$ was opened by Ref. [32], where the first NNLO QCD computation of the inclusive cross section was carried out. The main difficulty in any such calculation is the two-loop virtual amplitude, and the strategy followed in that work was to circumvent a direct computation by resorting to two complementary kinematic approximations: one in which the W boson is taken to be soft (SA), and another in which the top quark is treated as light relative to all remaining scales, i.e. a high-energy or massification limit (MA). Conservative error assessments indicated that the uncertainties stemming from these approximations were smaller than the residual scale dependence, yet verifying this conclusion with an explicit two-loop amplitude evaluation has remained an important open question.

In this contribution, based on the results reported in Ref. [33], I describe an NNLO QCD calculation where the two-loop amplitude for $t\bar{t}W$ is computed directly, for the first time, in the generalised leading-colour approximation (LCA). The LCA is fundamentally different from SA and MA: it is a parametric expansion governed by $1/N_c$, and does not invoke any kinematic extrapolation. The $2 \to 3$ scattering configuration, with massive top quarks in both the initial and final loop states, generates an extraordinary degree of algebraic complexity together with analytic structures — elliptic curves and nested square roots — that place this computation among the most demanding applications of state-of-the-art multi-loop technology. The NNLO cross sections obtained with the LCA are found to agree with those of Ref. [32], thereby providing an independent validation of the earlier approximate approach.

PoS(LL2026)055

2. Calculation

2.1 Organisation of the NNLO computation

The computational framework is built around the MATRIX code [34], which had been extended to $t\bar{t}W$ production in Ref. [32] following its successful application to several related channels [35–39]. IR singularities at NNLO are handled through q_T-subtraction [40], whose generalisation to processes involving heavy quarks was developed in Refs. [35, 36, 41]. The real-emission contribution $t\bar{t}W$ + jet is treated at NLO with dipole subtraction [42–44], while soft-parton terms specific to massive quarks are provided by the SHARK library [45, 46]. Tree-level and one-loop matrix elements needed throughout the calculation are supplied by OPENLOOPS [47–49].

Within the q_T-subtraction formalism, the double-virtual contribution enters the NNLO cross section via the hard coefficient $H^{(2)}$. This quantity is obtained by interefering the two-loop amplitude with the Born amplitude, carrying out UV renormalisation and subtracting the predicted IR singularities [50], and finally dividing by the squared Born matrix element. The one-loop amplitudes and the differential equations for the necessary master integrals were already worked out in Refs. [51, 52]. Hence $H^{(2)}$ constituted the sole missing ingredient, and its computation represents the central new result of this work.

2.2 Two-loop amplitude

The partonic channel under study is $u\,\bar{d} \to t\,\bar{t}\,W^+$, with the W^- case obtained by charge conjugation. Diagrams are produced with `QGRAF` [53], and the insertion of Feynman rules together with the colour-algebra decomposition is carried out in `FORM` [54, 55]. The set of diagrams is organised into 19 integral families, three of which are genuine two-loop families once crossing symmetries of the external legs are accounted for [52]; the rest reduce to products of one-loop integrals.

The calculation is performed in the LCA, retaining only the colour structures proportional to N_c^2, $N_c n_l$, and n_l^2, where $N_c = 3$ and $n_l = 5$ counts the massless flavours. In line with Ref. [51], we project the bare two-loop amplitude onto 24 independent tensor structures using the physical-projector technique [56, 57], working in the 't Hooft–Veltman scheme [58]. After projection, each amplitude is expressed as a linear combination of scalar Feynman integrals drawn from the families of Ref. [52] and their crossings, with rational-function coefficients.

This calculation faces two significant hurdles. The first concerns the Feynman integrals themselves. They contain elliptic curves and nested square roots [52], features that make a straightforward numerical evaluation over the full $2 \to 3$ phase space impractical. The strategy we adopt, following the methodology of Refs. [59, 60], is to expand the integral bases around $\epsilon = 0$ and express the coefficients through an (over-)complete set of special functions that obey a system of first-order algebraic partial differential equations. Numerical values for these special functions are obtained by solving the differential equations with AMFLOW's DE solver [61], using high-precision boundary conditions in the physical region also determined with AMFLOW [62]. An important advantage of this representation is that UV and IR poles can be subtracted analytically, after which the finite remainder takes the compact form of a linear combination of the special functions multiplied by rational coefficients. To make sure that the pole-subtraction ingredients all refer to the same basis, we recomputed the one-loop LCA amplitude and the mass-counterterm insertion in this framework

PoS(LL2026)055

and validated them against Ref. [51]. For a typical phase-space point, evaluating the full set of special functions takes between 20 and 120 CPU-minutes.

The second bottleneck is the size of the rational coefficients. To manage it, we perform all rational operations numerically over finite fields [63, 64], embedding the workflow in a FiniteFlow dataflow graph [65]. The required integration-by-parts reductions [66–68] are generated with NeatIBP [69], and the Laurent expansion in ϵ is performed within the same dataflow setup. We do not attempt to reconstruct the analytic expressions of the rational coefficients; instead, we evaluate them point by point over finite fields and lift the results to rational numbers through the Chinese remainder theorem [70]. Up to 400 finite-field primes are needed per phase-space point, depending on the kinematic configuration.

2.3 Numerical cross-check and interpolation

A fully independent numerical validation has been implemented. In this alternative setup, the unpolarised interference with the tree-level amplitude is computed in the conventional dimensional-regularisation scheme. Integral reduction relies on Blade [71], which builds a block-triangular IBP system [72]. The distinguishing feature of this cross-check is that the system is solved numerically with floating-point arithmetic at each point, thus entirely avoiding the finite-field reconstruction that the main approach requires. The basis integrals feeding this system are computed by solving the differential equations of Ref. [52] with AMFlow's DE solver [61]. Individual blocks contain $O(100)$ equations, so numerical error accumulation is not an issue. Additionally, the dimensional regulator ϵ is treated numerically: we fix $\epsilon = \pm\bar{\epsilon}$, where $\bar{\epsilon} = 1/1000$, and keep this numerical value throughout the entire calculation [73–75]. The finite remainder is then recovered by combining the two evaluations, with a residual uncertainty of $O(\bar{\epsilon}^2)$. The two computations agree to five significant digits at all benchmark points tested.

The two-loop finite remainder is sampled on a five-dimensional phase-space grid of 224,640 points, parameterised as suggested in Ref. [76] through two energy fractions and three angular variables. A few grid points suffer from strong numerical cancellations and are recomputed with elevated precision to guarantee at least five accurate digits throughout. The hard-virtual coefficient $H^{(2)}$ is then interpolated with quadratic B-splines. The one-loop validation of the interpolation yields sub-permille accuracy for the inclusive integral and percent-level accuracy for differential distributions (referenced to the full NLO cross section). At two loops, the integrated result is essentially insensitive to the precise interpolation scheme within the numerical integration errors.

3. Phenomenological results

3.1 Setup and comparison of approximations

Predictions refer to proton–proton collisions at $\sqrt{s} = 13\,\text{TeV}$, chosen to enable a side-by-side comparison with the results of Ref. [32]. The top-quark pole mass is fixed at $m_t = 173.2\,\text{GeV}$, the W-boson mass at $m_W = 80.385\,\text{GeV}$, and EW inputs follow the G_μ-scheme with a diagonal CKM matrix. We employ the `NNPDF31_nnlo_as_0118_luxqed` PDF set [77]. Central renormalisation and factorisation scales are $\mu_\text{R} = \mu_\text{F} = m_t + m_W/2$, and scale uncertainties are determined from the customary seven-point variation.

PoS(LL2026)055

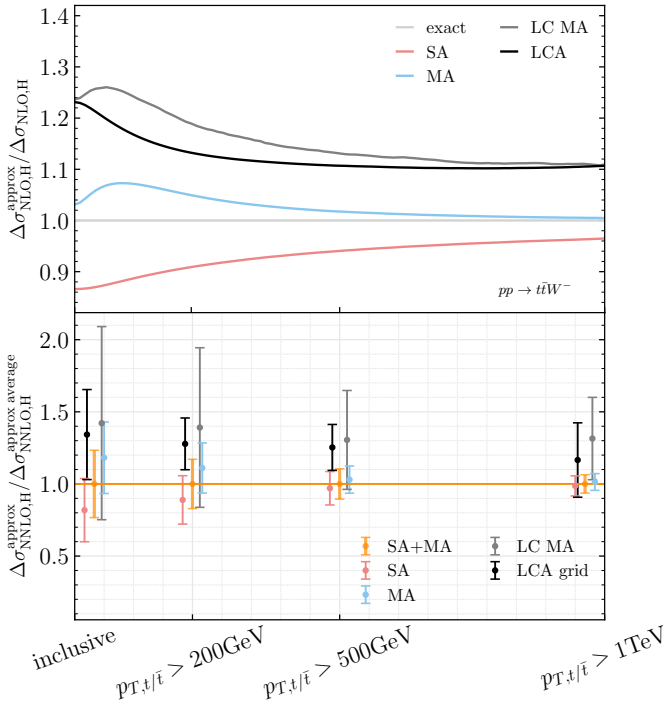

Figure 1: Results for $\Delta\sigma_{\text{NLO,H}}$ (upper panel) and $\Delta\sigma_{\text{NNLO,H}}$ (lower panel) in the case of $t\bar{t}W^-$ production, for the soft approximation (SA), massification approach (MA) and LCA, as functions of the lower cut applied to the transverse momenta of the top quarks. At NLO the approximations are normalised to the exact result, while at NNLO to the best result (SA+MA) from Ref. [32]. The uncertainties assigned to each approximation at NNLO are discussed in the text. Similar results are obtained for $t\bar{t}W^+$.

Figure 1 collects the NLO and NNLO hard-virtual contributions obtained with the LCA, plotted together with the SA and MA predictions of Ref. [32] as functions of a lower cut on $p_{T,t/\bar{t}}$. The SA corresponds to the limit of a soft W boson, whereas the MA exploits the high-energy regime where the top mass is negligible relative to all other scales, constructed via massification [78, 79]. Only the hard-virtual coefficient $H^{(n)}$ receives the approximation; the Born piece stays exact in all cases.

Looking first at the upper panel, which presents NLO predictions relative to the exact one-loop calculation, one observes the pattern established in Ref. [32]: SA falls below the exact curve, MA rises above it, and both converge toward the exact result when a hard cut is imposed on the top transverse momenta. In that large-$p_{T,t/\bar{t}}$ domain the MA reproduces the exact result at the percent level. The LCA behaviour is somewhat different — it overestimates the exact prediction by around 22% at the inclusive level, with this offset shrinking to roughly 10% at large $p_{T,t/\bar{t}}$. For large transverse momenta the LCA is in excellent agreement with its high-energy counterpart, the LC MA, recapitulating the trend observed for the full-colour case.

The lower panel turns to the NNLO comparison, where all curves are divided by the SA+MA central value from Ref. [32] (orange band). The SA+MA result was defined there as the arithmetic mean of the SA and MA predictions, with uncertainties combined linearly. The uncertainty assigned to each of these approximations was derived from its NLO performance: the relative uncertainty at NNLO was taken as twice the relative difference between the approximate and exact NLO results, a

PoS(LL2026)055

conservative rule motivated by the fact that SA and MA are dynamical approximations applied far outside the kinematic domains where they are formally justified. Variations of the IR subtraction scale $\mu_{\rm IR}$ around Q are also folded in.

3.2 Uncertainty estimate for the LCA

The situation is different for the LCA. Being a parametric expansion in $1/N_c$, it does not share the kinematic limitations of SA and MA; its main deficiency is expected to appear near the production threshold, where subleading-colour (SLC) effects become prominent. This kinematic region, however, makes a negligible contribution to the total cross section. Two empirical observations further support a reliable uncertainty estimate: at one loop, the difference between the exact and LCA coefficients shows negligible variation across phase space beyond the threshold region, and the ratio of the two-loop to one-loop LCA coefficients is similarly flat. These facts suggest that the relative one-loop difference provides a fair estimate of the missing SLC effects at two loops.

We therefore estimate the LCA uncertainty on $H^{(2)}$ from the relative discrepancy between the exact and LCA one-loop results. Shifting $\mu_{\rm IR}$ around Q produces only subleading effects. The numerical error introduced by the grid interpolation, which stays below 1% inclusively but grows to around 12% in the high-$p_{T,t/\bar{t}}$ region, is added linearly. The resulting LCA predictions (black markers in Fig. 1) lie systematically above the SA+MA reference, but the two uncertainty bands are fully compatible. Grey markers display the LC MA result, built from massless two-loop W + 4-parton amplitudes [80, 81] with the massification ingredients kept in LC.

3.3 Integrated cross sections

The inclusive numbers for the hard-virtual contribution $H^{(2)}$ are listed in Table 1.

	$t\bar{t}W^-$ [fb]	$t\bar{t}W^+$ [fb]
SA	15.67 (0) ± 4.21	34.59 (0) ± 9.18
MA	22.62(15) ± 4.78	49.87(40) ± 8.74
SA+MA	19.14 (8) ± 4.49	42.23(20) ± 8.96
LCA	25.70 (0) ± 5.68	56.76 (0) ± 12.03

Table 1: Contribution of $H^{(2)}$ to the inclusive NNLO cross section in the various approximations. The numbers in parentheses indicate the Monte Carlo integration error; the second uncertainty is the estimated uncertainty on each approximation. For SA and MA this estimate follows the prescription of Ref. [32]; for the LCA it also includes an estimate of the grid-interpolation error, as discussed in the text.

As expected from Fig. 1, the LCA values for $H^{(2)}$ are the largest among all approximations, but still consistent with the others inside the quoted errors. When the two-loop term is combined with the exactly computed remaining NNLO pieces, one arrives at the full NNLO QCD cross sections presented in Table 2.

The LCA-based central values exceed the SA+MA reference by approximately 3%, well within the respective uncertainties. Comparing with Table 1, the two-loop virtual contribution itself is substantial: it represents about 11% of the full NNLO cross section.

PoS(LL2026)055

	$t\bar{t}W^-$ [fb]	$t\bar{t}W^+$ [fb]
SA+MA [32]	$235.4\,(0)^{+5.1\%}_{-6.6\%} \pm 1.9\%$	$474.9\,(2)^{+4.8\%}_{-6.4\%} \pm 1.9\%$
LCA	$241.9\,(0)^{+6.4\%}_{-7.3\%} \pm 2.3\%$	$489.4\,(1)^{+6.3\%}_{-7.2\%} \pm 2.5\%$

Table 2: NNLO QCD cross sections. The perturbative uncertainties are estimated through standard seven-point scale variation. The additional uncertainty assigned to the SA+MA result corresponds to the approximation error estimated in Ref. [32]; for the LCA it accounts for the missing subleading-colour contributions and the grid-interpolation error, as discussed in the text.

4. Summary

This contribution has covered an NNLO QCD calculation of $t\bar{t}W$ hadroproduction where, for the first time, the two-loop virtual amplitudes are directly evaluated, in the generalised LCA. The full computation is documented in Ref. [33]. Carried out on a phase-space grid of more than 200,000 points using state-of-the-art multi-loop amplitude techniques, the calculation has been validated through a completely independent numerical approach.

The resulting NNLO cross sections fully corroborate the earlier determination of Ref. [32], which had relied on dynamical approximations of the two-loop contribution. The uncertainty associated with the unresolved subleading-colour pieces is estimated at roughly 2.5% — slightly above the previous estimate, yet still subdominant compared with scale variations. Going beyond the phenomenological impact, this work shows that numerical methods rooted in special-function representations have reached a level of maturity where they can be deployed in complete two-loop calculations for complex LHC final states. In the near term, the LCA results provide a basis for approximating the subleading-colour effects following the roadmap of Ref. [32], for which all the required building blocks are now in place.

Acknowledgments

I would like to thank M. Becchetti, D. Canko, V. Chestnov, M. Delto, S. Ditsch, M. Grazzini, S. Kallweit, T. Peraro, M. Pozzoli, C. Savoini, L. Tancredi, and S. Zoia for the excellent collaboration on which the results presented here are based. This work is supported by the Swiss National Science Foundation (SNSF) under contract 200020_219367, and by the UZH Postdoc Grant, grant No. [FK-25-104].

References

[1] **ATLAS** Collaboration, M. Aaboud et al., *Search for new phenomena in events with same-charge leptons and b-jets in pp collisions at $\sqrt{s}$ = 13 TeV with the ATLAS detector*, *JHEP* **12** (2018) 039, [arXiv:1807.11883].

[2] **ATLAS** Collaboration, G. Aad et al., *Search for squarks and gluinos in final states with same-sign leptons and jets using 139 fb^{-1} of data collected with the ATLAS detector*, *JHEP* **06** (2020) 046, [arXiv:1909.08457].

PoS(LL2026)055

[3] **CMS** Collaboration, A. M. Sirunyan et al., *Search for physics beyond the standard model in events with jets and two same-sign or at least three charged leptons in proton-proton collisions at $\sqrt{s}$ = 13 TeV*, *Eur. Phys. J. C* **80** (2020), no. 8 752, [arXiv:2001.10086].

[4] **ATLAS** Collaboration, G. Aad et al., *Measurement of the $t\bar{t}W$ and $t\bar{t}Z$ production cross sections in pp collisions at $\sqrt{s}$ = 8 TeV with the ATLAS detector*, *JHEP* **11** (2015) 172, [arXiv:1509.05276].

[5] **CMS** Collaboration, V. Khachatryan et al., *Observation of top quark pairs produced in association with a vector boson in pp collisions at $\sqrt{s}$ = 8 TeV*, *JHEP* **01** (2016) 096, [arXiv:1510.01131].

[6] **ATLAS** Collaboration, M. Aaboud et al., *Measurement of the $t\bar{t}Z$ and $t\bar{t}W$ production cross sections in multilepton final states using 3.2 fb^{-1} of pp collisions at $\sqrt{s}$ = 13 TeV with the ATLAS detector*, *Eur. Phys. J. C* **77** (2017), no. 1 40, [arXiv:1609.01599].

[7] **CMS** Collaboration, A. M. Sirunyan et al., *Measurement of the cross section for top quark pair production in association with a W or Z boson in proton-proton collisions at $\sqrt{s}$ = 13 TeV*, *JHEP* **08** (2018) 011, [arXiv:1711.02547].

[8] **ATLAS** Collaboration, M. Aaboud et al., *Measurement of the $t\bar{t}Z$ and $t\bar{t}W$ cross sections in proton-proton collisions at $\sqrt{s}$ = 13 TeV with the ATLAS detector*, *Phys. Rev. D* **99** (2019), no. 7 072009, [arXiv:1901.03584].

[9] **ATLAS** Collaboration, *Measurement of the total and differential cross-sections of $t\bar{t}W$ production in pp collisions at 13 TeV with the ATLAS detector*, .

[10] **ATLAS** Collaboration, G. Aad et al., *Measurement of the total and differential cross-sections of $t\bar{t}W$ production in pp collisions at $\sqrt{s}$ = 13 TeV with the ATLAS detector*, *JHEP* **05** (2024) 131, [arXiv:2401.05299]. [Erratum: JHEP 11, 127 (2025)].

[11] **CMS** Collaboration, A. Tumasyan et al., *Measurement of the cross section of top quark-antiquark pair production in association with a W boson in proton-proton collisions at $\sqrt{s}$ = 13 TeV*, *JHEP* **07** (2023) 219, [arXiv:2208.06485].

[12] **CMS** Collaboration, A. Hayrapetyan et al., *Measurements of $t\bar{t}W$ differential cross sections and the leptonic charge asymmetry at $\sqrt{s}$ = 13 TeV*, *JHEP* **03** (2026) 083, [arXiv:2509.13512].

[13] **ATLAS** Collaboration, *Analysis of $t\bar{t}H$ and $t\bar{t}W$ production in multilepton final states with the ATLAS detector*, .

[14] **CMS** Collaboration, A. M. Sirunyan et al., *Measurement of the Higgs boson production rate in association with top quarks in final states with electrons, muons, and hadronically decaying tau leptons at $\sqrt{s}$ = 13 TeV*, *Eur. Phys. J. C* **81** (2021), no. 4 378, [arXiv:2011.03652].

PoS(LL2026)055

[15] **CMS** Collaboration, A. Hayrapetyan et al., *Observation of four top quark production in proton-proton collisions at $\sqrt{s}$ = 13 TeV*, *Phys. Lett. B* **847** (2023) 138290, [arXiv:2305.13439].

[16] **ATLAS** Collaboration, G. Aad et al., *Observation of four-top-quark production in the multilepton final state with the ATLAS detector*, *Eur. Phys. J. C* **83** (2023), no. 6 496, [arXiv:2303.15061]. [Erratum: Eur.Phys.J.C 84, 156 (2024)].

[17] S. Badger, J. M. Campbell, and R. K. Ellis, *QCD Corrections to the Hadronic Production of a Heavy Quark Pair and a W-Boson Including Decay Correlations*, *JHEP* **03** (2011) 027, [arXiv:1011.6647].

[18] J. M. Campbell and R. K. Ellis, *$t\bar{t}W^{+-}$ production and decay at NLO*, *JHEP* **07** (2012) 052, [arXiv:1204.5678].

[19] F. Maltoni, D. Pagani, and I. Tsinikos, *Associated production of a top-quark pair with vector bosons at NLO in QCD: impact on* $\mathrm{t\bar{t}H}$ *searches at the LHC*, *JHEP* **02** (2016) 113, [arXiv:1507.05640].

[20] S. Frixione, V. Hirschi, D. Pagani, H. S. Shao, and M. Zaro, *Electroweak and QCD corrections to top-pair hadroproduction in association with heavy bosons*, *JHEP* **06** (2015) 184, [arXiv:1504.03446].

[21] R. Frederix, D. Pagani, and M. Zaro, *Large NLO corrections in $t\bar{t}W^{\pm}$ and $t\bar{t}t\bar{t}$ hadroproduction from supposedly subleading EW contributions*, *JHEP* **02** (2018) 031, [arXiv:1711.02116].

[22] H. T. Li, C. S. Li, and S. A. Li, *Renormalization group improved predictions for $t\bar{t}W^{\pm}$ production at hadron colliders*, *Phys. Rev. D* **90** (2014), no. 9 094009, [arXiv:1409.1460].

[23] A. Broggio, A. Ferroglia, G. Ossola, and B. D. Pecjak, *Associated production of a top pair and a W boson at next-to-next-to-leading logarithmic accuracy*, *JHEP* **09** (2016) 089, [arXiv:1607.05303].

[24] A. Kulesza, L. Motyka, D. Schwartländer, T. Stebel, and V. Theeuwes, *Associated production of a top quark pair with a heavy electroweak gauge boson at NLO+NNLL accuracy*, *Eur. Phys. J. C* **79** (2019), no. 3 249, [arXiv:1812.08622].

[25] A. Broggio, A. Ferroglia, R. Frederix, D. Pagani, B. D. Pecjak, and I. Tsinikos, *Top-quark pair hadroproduction in association with a heavy boson at NLO+NNLL including EW corrections*, *JHEP* **08** (2019) 039, [arXiv:1907.04343].

[26] G. Bevilacqua, H.-Y. Bi, H. B. Hartanto, M. Kraus, and M. Worek, *The simplest of them all: $t\bar{t}W^{\pm}$ at NLO accuracy in QCD*, *JHEP* **08** (2020) 043, [arXiv:2005.09427].

[27] A. Denner and G. Pelliccioli, *NLO QCD corrections to off-shell $t\bar{t}W^{+}$ production at the LHC*, *JHEP* **11** (2020) 069, [arXiv:2007.12089].

PoS(LL2026)055

[28] G. Bevilacqua, H.-Y. Bi, H. B. Hartanto, M. Kraus, J. Nasufi, and M. Worek, *NLO QCD corrections to off-shell $t\bar{t}W^{\pm}$ production at the LHC: correlations and asymmetries*, *Eur. Phys. J. C* **81** (2021), no. 7 675, [arXiv:2012.01363].

[29] A. Denner and G. Pelliccioli, *Combined NLO EW and QCD corrections to off-shell $t\bar{t}W$ production at the LHC*, *Eur. Phys. J. C* **81** (2021), no. 4 354, [arXiv:2102.03246].

[30] R. Frederix and S. Frixione, *Merging meets matching in MC@NLO*, *JHEP* **12** (2012) 061, [arXiv:1209.6215].

[31] R. Frederix and I. Tsinikos, *On improving NLO merging for* $\mathrm{t\bar{t}W}$ *production*, *JHEP* **11** (2021) 029, [arXiv:2108.07826].

[32] L. Buonocore, S. Devoto, M. Grazzini, S. Kallweit, J. Mazzitelli, L. Rottoli, and C. Savoini, *Precise Predictions for the Associated Production of a W Boson with a Top-Antitop Quark Pair at the LHC*, *Phys. Rev. Lett.* **131** (2023), no. 23 231901, [arXiv:2306.16311].

[33] M. Becchetti, D. Canko, X. Chen, V. Chestnov, M. Delto, S. Ditsch, M. Grazzini, S. Kallweit, T. Peraro, M. Pozzoli, C. Savoini, L. Tancredi, and S. Zoia, *NNLO QCD predictions for $t\bar{t}W$ production at hadron colliders*, arXiv:2606.09503.

[34] M. Grazzini, S. Kallweit, and M. Wiesemann, *Fully differential NNLO computations with MATRIX*, *Eur. Phys. J. C* **78** (2018), no. 7 537, [arXiv:1711.06631].

[35] S. Catani, S. Devoto, M. Grazzini, S. Kallweit, J. Mazzitelli, and H. Sargsyan, *Top-quark pair hadroproduction at next-to-next-to-leading order in QCD*, *Phys. Rev. D* **99** (2019), no. 5 051501, [arXiv:1901.04005].

[36] S. Catani, S. Devoto, M. Grazzini, S. Kallweit, and J. Mazzitelli, *Top-quark pair production at the LHC: Fully differential QCD predictions at NNLO*, *JHEP* **07** (2019) 100, [arXiv:1906.06535].

[37] S. Catani, S. Devoto, M. Grazzini, S. Kallweit, and J. Mazzitelli, *Bottom-quark production at hadron colliders: fully differential predictions in NNLO QCD*, *JHEP* **03** (2021) 029, [arXiv:2010.11906].

[38] L. Buonocore, S. Devoto, S. Kallweit, J. Mazzitelli, L. Rottoli, and C. Savoini, *Associated production of a W boson and massive bottom quarks at next-to-next-to-leading order in QCD*, *Phys. Rev. D* **107** (2023), no. 7 074032, [arXiv:2212.04954].

[39] S. Devoto, M. Grazzini, S. Kallweit, J. Mazzitelli, and C. Savoini, *Precise predictions for $t\bar{t}H$ production at the LHC: inclusive cross section and differential distributions*, *JHEP* **03** (2025) 189, [arXiv:2411.15340].

[40] S. Catani and M. Grazzini, *An NNLO subtraction formalism in hadron collisions and its application to Higgs boson production at the LHC*, *Phys. Rev. Lett.* **98** (2007) 222002, [hep-ph/0703012].

PoS(LL2026)055

[41] R. Bonciani, S. Catani, M. Grazzini, H. Sargsyan, and A. Torre, *The q_T subtraction method for top quark production at hadron colliders*, *Eur. Phys. J. C* **75** (2015), no. 12 581, [arXiv:1508.03585].

[42] S. Catani and M. H. Seymour, *The Dipole formalism for the calculation of QCD jet cross-sections at next-to-leading order*, *Phys. Lett. B* **378** (1996) 287–301, [hep-ph/9602277].

[43] S. Catani and M. H. Seymour, *A General algorithm for calculating jet cross-sections in NLO QCD*, *Nucl. Phys. B* **485** (1997) 291–419, [hep-ph/9605323]. [Erratum: Nucl.Phys.B 510, 503–504 (1998)].

[44] S. Catani, S. Dittmaier, M. H. Seymour, and Z. Trocsanyi, *The Dipole formalism for next-to-leading order QCD calculations with massive partons*, *Nucl. Phys. B* **627** (2002) 189–265, [hep-ph/0201036].

[45] S. Catani, S. Devoto, M. Grazzini, and J. Mazzitelli, *Soft-parton contributions to heavy-quark production at low transverse momentum*, *JHEP* **04** (2023) 144, [arXiv:2301.11786].

[46] S. Devoto and J. Mazzitelli, *Soft contributions to heavy quark production in arbitrary kinematics*, arXiv:2509.17509.

[47] F. Cascioli, P. Maierhöfer, and S. Pozzorini, *Scattering Amplitudes with Open Loops*, *Phys. Rev. Lett.* **108** (2012) 111601, [arXiv:1111.5206].

[48] F. Buccioni, S. Pozzorini, and M. Zoller, *On-the-fly reduction of open loops*, *Eur. Phys. J. C* **78** (2018), no. 1 70, [arXiv:1710.11452].

[49] F. Buccioni, J.-N. Lang, J. M. Lindert, P. Maierhöfer, S. Pozzorini, H. Zhang, and M. F. Zoller, *OpenLoops 2*, *Eur. Phys. J. C* **79** (2019), no. 10 866, [arXiv:1907.13071].

[50] A. Ferroglia, M. Neubert, B. D. Pecjak, and L. L. Yang, *Two-loop divergences of massive scattering amplitudes in non-abelian gauge theories*, *JHEP* **11** (2009) 062, [arXiv:0908.3676].

[51] M. Becchetti, M. Delto, S. Ditsch, P. A. Kreer, M. Pozzoli, and L. Tancredi, *One-loop QCD corrections to $\bar{u}d \to t\bar{t}W$ at $O\left(\varepsilon^2\right)$*, *JHEP* **09** (2025) 126, [arXiv:2502.14952].

[52] M. Becchetti, D. Canko, V. Chestnov, T. Peraro, M. Pozzoli, and S. Zoia, *Two-loop Feynman integrals for leading colour $t\bar{t}W$ production at hadron colliders*, *JHEP* **07** (2025) 001, [arXiv:2504.13011].

[53] P. Nogueira, *Automatic Feynman Graph Generation*, *J. Comput. Phys.* **105** (1993) 279–289.

[54] B. Ruijl, T. Ueda, and J. Vermaseren, *FORM version 4.2*, arXiv:1707.06453.

[55] J. Davies, T. Kaneko, C. Marinissen, T. Ueda, and J. A. M. Vermaseren, *FORM Version 5.0*, arXiv:2601.19982.

PoS(LL2026)055

[56] T. Peraro and L. Tancredi, *Physical projectors for multi-leg helicity amplitudes*, *JHEP* **07** (2019) 114, [arXiv:1906.03298].

[57] T. Peraro and L. Tancredi, *Tensor decomposition for bosonic and fermionic scattering amplitudes*, *Phys. Rev. D* **103** (2021), no. 5 054042, [arXiv:2012.00820].

[58] G. 't Hooft and M. J. G. Veltman, *Regularization and Renormalization of Gauge Fields*, *Nucl. Phys. B* **44** (1972) 189–213.

[59] S. Badger, M. Becchetti, C. Brancaccio, H. B. Hartanto, and S. Zoia, *Numerical evaluation of two-loop QCD helicity amplitudes for $gg \to t\bar{t}g$ at leading colour*, *JHEP* **03** (2025) 070, [arXiv:2412.13876].

[60] S. Badger, M. Becchetti, C. Brancaccio, M. Czakon, H. B. Hartanto, R. Poncelet, and S. Zoia, *Double virtual QCD corrections to $t\bar{t}$+jet production at the LHC*, arXiv:2511.11424.

[61] X. Liu and Y.-Q. Ma, *AMFlow: A Mathematica package for Feynman integrals computation via auxiliary mass flow*, *Comput. Phys. Commun.* **283** (2023) 108565, [arXiv:2201.11669].

[62] X. Liu, Y.-Q. Ma, and C.-Y. Wang, *A Systematic and Efficient Method to Compute Multi-loop Master Integrals*, *Phys. Lett. B* **779** (2018) 353–357, [arXiv:1711.09572].

[63] A. von Manteuffel and R. M. Schabinger, *A novel approach to integration by parts reduction*, *Phys. Lett. B* **744** (2015) 101–104, [arXiv:1406.4513].

[64] T. Peraro, *Scattering amplitudes over finite fields and multivariate functional reconstruction*, *JHEP* **12** (2016) 030, [arXiv:1608.01902].

[65] T. Peraro, *FiniteFlow: multivariate functional reconstruction using finite fields and dataflow graphs*, *JHEP* **07** (2019) 031, [arXiv:1905.08019].

[66] F. V. Tkachov, *A theorem on analytical calculability of 4-loop renormalization group functions*, *Phys. Lett. B* **100** (1981) 65–68.

[67] K. G. Chetyrkin and F. V. Tkachov, *Integration by parts: The algorithm to calculate β-functions in 4 loops*, *Nucl. Phys. B* **192** (1981) 159–204.

[68] S. Laporta, *High-precision calculation of multiloop Feynman integrals by difference equations*, *Int. J. Mod. Phys. A* **15** (2000) 5087–5159, [hep-ph/0102033].

[69] Z. Wu, J. Boehm, R. Ma, H. Xu, and Y. Zhang, *NeatIBP 1.0, a package generating small-size integration-by-parts relations for Feynman integrals*, *Comput. Phys. Commun.* **295** (2024) 108999, [arXiv:2305.08783].

[70] T. Peraro, *Analytic multi-loop results using finite fields and dataflow graphs with FiniteFlow*, in *14th International Symposium on Radiative Corrections: Application of Quantum Field Theory to Phenomenology*, 12, 2019. arXiv:1912.03142.

PoS(LL2026)055

[71] X. Guan, X. Liu, Y.-Q. Ma, and W.-H. Wu, *Blade: A package for block-triangular form improved Feynman integrals decomposition*, *Comput. Phys. Commun.* **310** (2025) 109538, [arXiv:2405.14621].

[72] X. Guan, X. Liu, and Y.-Q. Ma, *Complete reduction of integrals in two-loop five-light-parton scattering amplitudes*, *Chin. Phys. C* **44** (2020), no. 9 093106, [arXiv:1912.09294].

[73] H.-Y. Bi, L.-H. Huang, R.-J. Huang, Y.-Q. Ma, and H.-M. Yu, *Electroweak Corrections to Double Higgs Production at the LHC*, *Phys. Rev. Lett.* **132** (2024), no. 23 231802, [arXiv:2311.16963].

[74] H.-Y. Bi, Y.-Q. Ma, and D.-M. Mu, *Electroweak loop corrections to $gg \to gH$ at the LHC*, *JHEP* **04** (2026) 087, [arXiv:2508.02588].

[75] H. T. Li, Y.-Q. Ma, C.-T. Tan, J. Wang, and H.-F. Zhang, *Compton-Scattering Total Cross Section at Next-to-Next-to-Leading Order and Resummation of Leading Logarithms*, *Phys. Rev. Lett.* **136** (2026), no. 2 021802, [arXiv:2511.09330].

[76] B. Agarwal, G. Heinrich, S. P. Jones, M. Kerner, S. Y. Klein, J. Lang, V. Magerya, and A. Olsson, *Two-loop amplitudes for $t\bar{t}H$ production: the quark-initiated N_f-part*, *JHEP* **05** (2024) 013, [arXiv:2402.03301]. [Erratum: JHEP 06, 142 (2024)].

[77] **NNPDF** Collaboration, V. Bertone, S. Carrazza, N. P. Hartland, and J. Rojo, *Illuminating the photon content of the proton within a global PDF analysis*, *SciPost Phys.* **5** (2018), no. 1 008, [arXiv:1712.07053].

[78] A. Mitov and S. Moch, *The Singular behavior of massive QCD amplitudes*, *JHEP* **05** (2007) 001, [hep-ph/0612149].

[79] G. Wang, T. Xia, L. L. Yang, and X. Ye, *On the high-energy behavior of massive QCD amplitudes*, *JHEP* **05** (2024) 082, [arXiv:2312.12242].

[80] S. Abreu, F. Febres Cordero, H. Ita, M. Klinkert, B. Page, and V. Sotnikov, *Leading-color two-loop amplitudes for four partons and a W boson in QCD*, *JHEP* **04** (2022) 042, [arXiv:2110.07541].

[81] S. Badger, H. B. Hartanto, and S. Zoia, *Two-Loop QCD Corrections to $Wb\bar{b}$ Production at Hadron Colliders*, *Phys. Rev. Lett.* **127** (2021), no. 1 012001, [arXiv:2102.02516].

PoS(LL2026)055